Otology & Neurotology
31:1199–1206 © 2010, Otology & Neurotology, Inc.

Inroads Toward Robot-Assisted Cochlear Implant Surgery Using Steerable Electrode Arrays

*Jian Zhang, *Wei Wei, *Jienan Ding, †J. Thomas Roland, Jr., ‡Spiros Manolidis, and *Nabil Simaan

**Department of Mechanical Engineering, Columbia University; †Department of Otolaryngology and Neurosurgery, New York University School of Medicine; and ‡Beth Israel Medical Center, New York, New York, U.S.A.*

Hypothesis: Robotic insertions of actively steerable perimodiolar electrode arrays can substantially reduce insertion forces and prevent electrode buckling.
Background: Perimodiolar electrodes have been proven to be effective in reducing insertion forces. However, the dedicated techniques of atraumatic electrode insertion require intensive surgeon training. Although some specialized medical robots have been developed to help surgeons in certain minimally invasive surgeries, none are applicable to electrode insertions.
Methods: A robot prototype capable of automatically inserting novel steerable electrode array and adjusting its approach angle toward the scala tympani has been constructed and tested. Comparisons of insertion forces using robotically assisted steerable and straight electrodes on scala tympani models are presented. Simulations and experiments are conducted to compare the robotic insertion outcomes and insertion forces.
Results: The use of robotically assisted steerable electrodes for insertions significantly reduces the insertion forces compared with straight electrodes. Based on the results from the experiments, a second-generation robot with insertion force-sensing capability and haptic control to be used in the operating room has been designed for cochlear implant surgery.
Conclusion: Preliminary experimental results using robot-assisted steerable electrode prototype show that it is effective in reducing insertion forces and preventing electrode buckling. A second-generation robot has been designed and constructed for cochlear implant surgery under operating room conditions.
Key Words: Cochlear implant—Robotic assistance—Steerable electrode—Trauma.

Otol Neurotol **31:**1199–1206, 2010.

Cochlear implantation is an accepted medical treatment of choice for the rehabilitation of congenital and acquired sensorineural hearing loss. The surgical procedure requires that an electrode be inserted into the cochlea to directly stimulate the spiral ganglion cells and provide auditory information to the central auditory pathways. More recently, and coincident with the development of more atraumatic electrodes and insertion techniques, there is great interest in implanting patients with more residual hearing (1,2). Additionally, recent studies (3) confirm that patients are able to use even small amounts of residual hearing effectively to hear better in noisy environments, appreciate music, and have better overall auditory performance.

Address correspondence and reprint requests to Nabil Simaan, Ph.D., Rm 234 S.W. Mudd Building, 500 W 120th Street, New York, NY 10027; E-mail: ns2236@columbia.edu
Sources of support that require acknowledgment: This work is funded by National Science Foundation Grant No. 0651649.

Existing electrode products include external-wall or straight electrodes, that is, C40+ electrode (MedEl, Innsbruck, Austria) and K electrode (Cochlear Corp., Englewood, CO, USA). During insertions, straight electrodes first make contact with the outer wall of the cochlea at approximately 180 degrees of insertion, which corresponds to the mid pars ascendens. After the first contact, the electrodes slide against the external wall and bend as more insertion pressure is exerted on the electrode to overcome frictional forces and stiffness properties of the electrode array to follow the curvature of the scala tympani (4,5). Direct contact with the external wall results in high cumulative friction forces in a manner similar to the application of a band break (6). Some buckling of the electrode typically occurs because of large insertion forces, and this, combined with upward forces that are generated, result in intracochlear trauma (7–10).

Alternatively, perimodiolar electrodes have been developed, that is, Contour Advance electrode (Cochlear Corp.) and HiFocus Helix Electrode (Advanced Bionics Corp.,

Sylmar, CA, USA). These electrodes have self-coiling properties and are straightened by metal stylets inserted in them. During surgery, the surgeon pulls out the stylet while inserting the electrode in a coordinated motion such that the electrode tip advances and coils toward the modiolus. The stylet serves the purpose of straightening and supporting the electrode. Perimodiolar electrodes are modiolus hugging, and therefore, the electrodes stay in a proximity to ganglion cells. Compared with straight electrodes, insertions of perimodiolar electrodes with proper techniques result in little force on the outer wall of the cochlea and therefore less resultant intracochlear trauma (11). However, tip foldovers, improper insertion techniques, and over-insertion have occurred (12). The majority of electrode insertions are operated without fluoroscopic imaging during operations. Therefore, markers on existing perimodiolar electrodes are used to guide surgeons in determining the appropriate electrode insertion depth and stylet retraction time during insertions. There is great variation in insertion technique among surgeons, and therefore, precise and atraumatic placement is not always achieved. As the technique only allows for advancing off the stylet, variations in technique and adaptation for a challenging insertion is not possible. Additionally, the electrodes are designed for the average-sized cochleae and are not always appropriately placed.

Although inserting straight electrodes does not require more than a pair of forceps, special tools are recommended to complete the complicated procedure of inserting perimodiolar electrodes. Advanced Bionics Corporation delivered a special tool set for inserting their HiFocus Helix Electrode. Cochlear Inc. exhibited their dedicated tool for Contour Advance electrode (13) but never released it in the United States. The use of these tools helps surgeons complete the insertions but still requires intensive training. In addition, use of these tools further hinders insertion force sensing and provides insufficient insertion force feedback to surgeons, which limits their ability to prevent excessive insertion forces and intracochlear trauma.

To improve surgical outcomes, medical robots are available for many minimally invasive operations (14,15). Although a few computer-aided medical devices have been designed for cochlear implant operations, the majority of them focus on drilling mastoid bones (16,18) and reconstructing 3-dimensional (3D) anatomies (19). The first work on robot-assisted electrode insertions with force-sensing capability was proposed in 2006 (20) and expanded in 2009 (21). The work (20) also designed a steerable electrode prototype to further improve the results of using robotic insertions. Later in 2006, a similar steerable electrode design actuated by Shape Memory Alloys was presented (22). In 2009, another robotic insertion tool specialized for Contour Advance electrode was introduced (23) but did not incorporate any force-sensing capability on the tool. The limitations of these prototypes include the following: only working with a special kind of electrodes (23), limited degrees of freedom (DoF) (23), and not applicable to real surgical procedures (21).

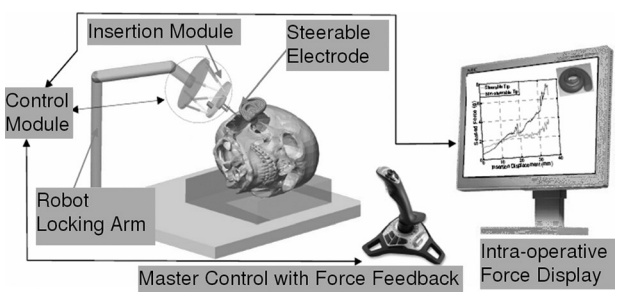

FIG. 1. Overview of robotic system for cochlear implant operations.

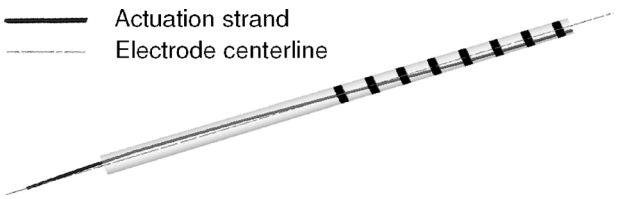

FIG. 2. Structure of a steerable electrode array.

This article presents results on robot-assisted electrode insertions and a second-generation robot designed to be used in the operating room. We think robotic insertions will achieve proper and precise electrode placement with less intracochlear trauma. Our preliminary results were detailed in (21), and in this article, we briefly outline some of the important results. To conduct better insertions, a novel actively steerable perimodiolar electrode array has been proposed and used in combination with a prototype robot. Robotic insertion method is discussed, simulated, and tested. Based on the results using the prototype robot, a second-generation parallel robot with force-sensing capability is designed and constructed as part of our ongoing work on constructing a telemanipulation system for cochlear implant surgery. This robot is designed for clinical application and aims to adapt various straight and perimodiolar electrodes (Fig. 1).

MATERIALS AND METHODS

Steerable Electrode Array and Scala Tympani Model

A new design of actively steerable electrode was proposed where a strand is embedded inside an elastomeric electrode array. Figure 2 shows the structure of the electrode array, which can be molded using any biocompatible silicone rubber. The embedded strand in the electrode is purposely placed off the centerline of the electrode and attached internally to the tip of the electrode. The rest of the strand can move inside the electrode. When pulling the strand while holding the base of the electrode array, the electrode array bends to predetermined shapes (Fig. 3). For proof of feasibility, we molded a 3:1 scaled-up electrode prototype shown in Figure 3 while avoiding unnecessary fabrication cost associated with a 1:1 prototype. Later, we fabricated a 1:1 steerable electrode prototype as shown in Figure 4.

The shape of the scala tympani central curve was summarized by Cohen et al. (24) using a planar curve. This shape was subsequently extended to 3D by Ketten et al. (25) and Yoo et al. (26). Both the planar and the 3D curves of the scala tympani

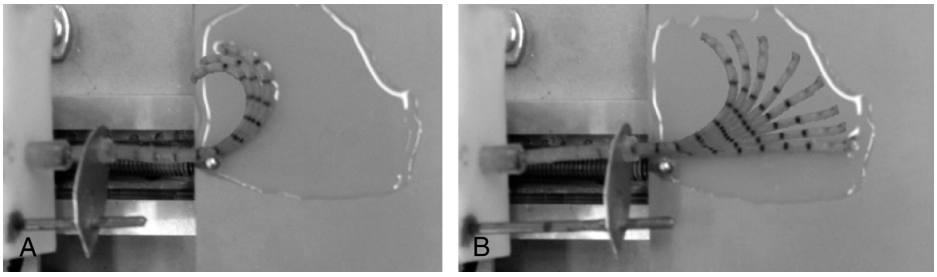

FIG. 3. Different shapes of bent steerable electrode array. *A*, Large amount of pull. *B*, Small amount of pull.

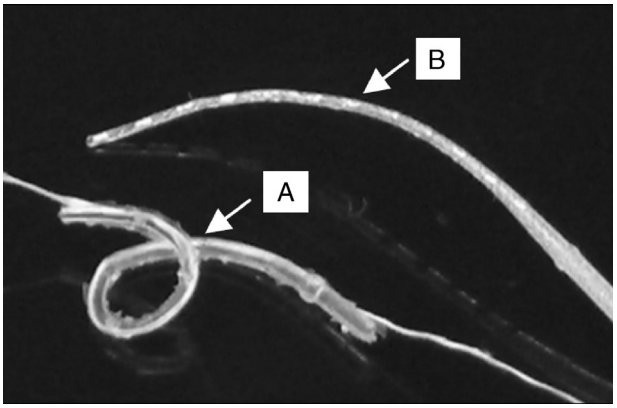

FIG. 4. *A*, 1:1 Steerable electrode array prototype. *B*, MedEl C40+ electrode.

were used for evaluation of robot-assisted insertions of the steerable electrode array in Figure 3. Figure 5A shows the planar acrylic model, and Figure 5B shows a 3D plastic model of the scala tympani. The cross-sectional dimensions of the scala tympani model were based on the results of Wysocki (27). To match the size of the steerable electrode array, both of these 2 models were scaled up by a factor of 3.

Robot Design and Insertion Method

The steerable electrode shown in Figure 3 offers the advantages of improved steerability. With robotic assistance, the steerable electrode steering includes 2 levels of motions. First, the electrode itself can be bent to a certain shape by the embedded strand (Fig. 3). Different amounts of pull on the strand (denoted as q_1) correspond to different bent shapes of the steerable electrode. This one-to-one correspondence is guaranteed by the elastic properties of the electrode. We have a mathematical model to predict all possible bent shapes of the electrode array (20).

Second, the bent electrode as a whole unit can be rotated by the robot, which further increases its steerability. The rotation from the robot can adjust the electrode approach angle toward the scala tympani. The robot prototype we constructed has 4 actuators as shown in Figure 6. The first actuator (denoted as q_2) moves the electrode forward and backward. The second actuator (denoted as q_1) pulls on the strand. The third actuator (denoted as q_3) adjusts the approach angle to the scala tympani by rotating

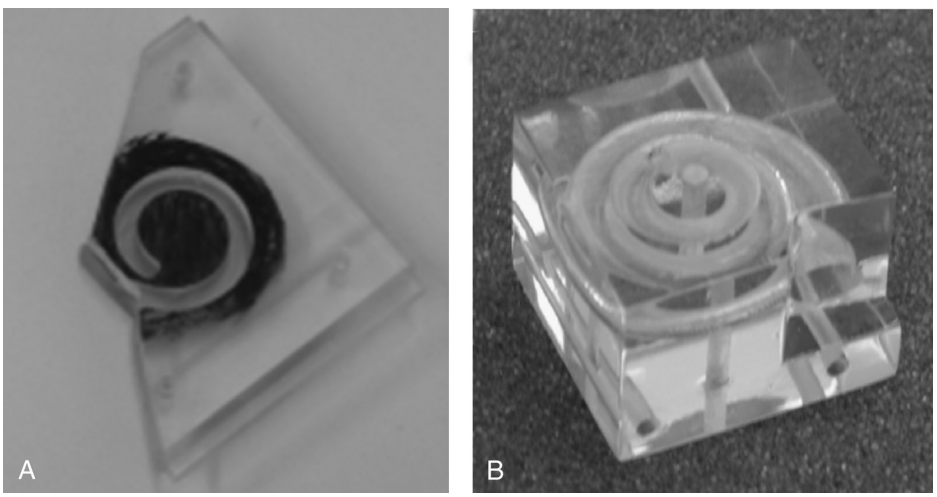

FIG. 5. Plastic scala tympani models. *A*, Planar model. *B*, 3D model.

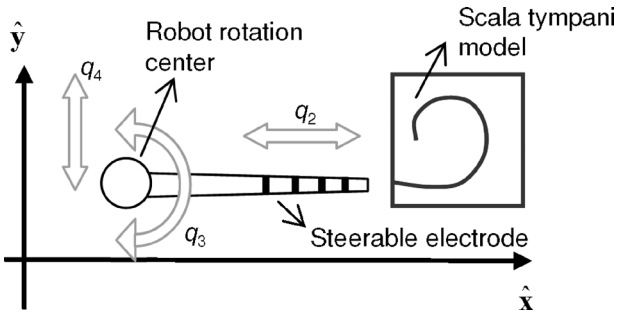

FIG. 6. Four DoF robot structure.

the robot. The fourth actuator (denoted as q_4) moves the robot sideways.

We designed a more advanced robot with force-sensing capability, and it can provide insertion force feedback to surgeons through a haptic device based on the results using the above robot prototype. The second-generation robot with haptic control is presented in the results section.

One hypothesis we assumed is that only when the bent electrode array shape matches the scala tympani curve, there will be no contact between the bent electrode and the external wall of the scala tympani so that the sensed insertion force will be minimized. The robotic electrode insertion strategy calculates the synchronized motions between 4 actuators of the robot.

Based on the planar scala tympani model curve, we compared robotic insertions without adjusting the approach angle (uses only 2 actuators, denoted as 2 DoF robot) and with adjusting the approach angle (uses 4 actuators, denoted as 4 DoF robot). Figure 7 shows a series of images at different insertion depths. Each subimage is an overlay of the scala tympani curve, the bent electrode using a 2 DoF robot, and the bent and rotated electrode using the 4 DoF robot. It is evident from the simulation that the 4 DoF robot achieves better shape match between the bent electrode and the scala tympani.

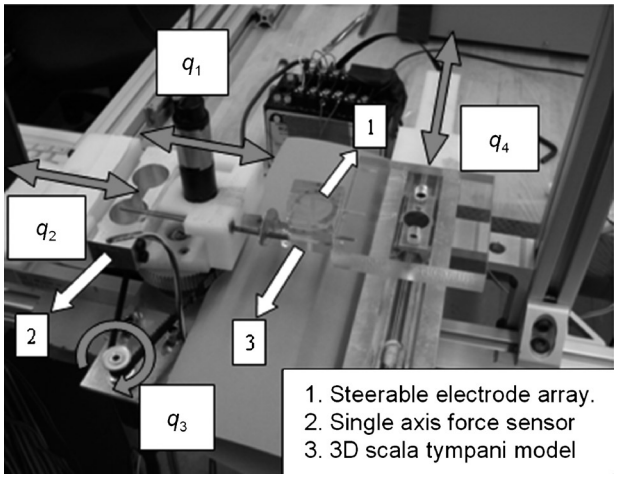

FIG. 8. Four DoF electrode insertion robot prototype.

Experimental Setup

The experiments were performed using the prototype robot shown in Figure 8. All the experimental data presented in the article were collected using this robot. Four precision gearmotors were selected to actuate the robot. When only actuating motors q_1 and q_2, the robot performs as a 2 DoF robot, which can only move forward and backward relatively to the scala tympani and simultaneously pull on the strand. If all 4 actuators are used, the same robot performs as a 4 DoF robot by providing 2 additional motions: adjusting the approach angle to the scala tympani and moving forward and backward along the electrode insertion direction.

A precise force sensor capable of detecting ±0.1 g forces was installed on the robot. The robot was controlled using Linux operating system with a Pentium-4 2.8 GHz CPU. This configuration makes it possible for the user to monitor the robot status in real time. Before insertions, glycerin was injected into

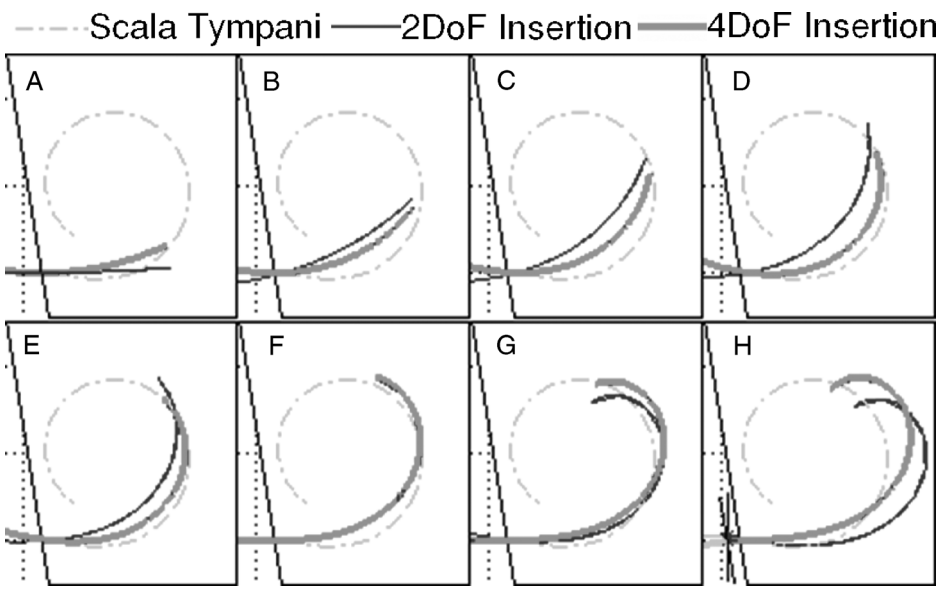

FIG. 7. Comparison between simulated 2 DoF and 4 DoF insertions.

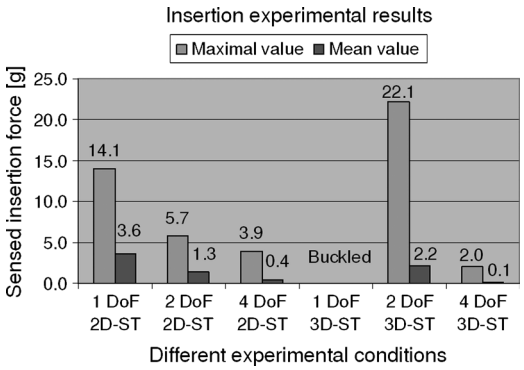

FIG. 9. Comparison of insertion results using different experimental conditions. ST indicates scala tympani.

the scala tympani models and served as lubricant for all experiments. When using the 3D scala tympani model, the electrode bending plane was tilted such that it matched the 3D helical angle of the scala tympani.

RESULTS

Experimental Results

Several groups of experiments were conducted to compare the insertion forces. A summary on insertion forces under different experimental conditions is presented in Figure 9. Under all insertion conditions, a minimal number of 3 trials were conducted to show repeatability.

Straight and steerable electrodes were robotically inserted into the planar and 3D scala tympani models. When inserting the steerable electrode into planar scala tympani model, the maximal insertion force was reduced by 59.6%. When inserting straight and steerable electrodes into the 3D scala tympani model, buckling occurred to the straight electrode. This buckling is captured by insertion images shown in Figure 10A3 and A4. Comparing Figure 10A and B, another noticeable difference is that the steerable electrode hugs more toward the modiolus during insertions.

Electrode insertions with the 4 DoF robot maintained much smaller insertion forces compared with 2 DoF robot. This result validates our assumption and the results from simulations. It also signifies that adjusting the electrode approach angle is important for reducing the insertion forces.

Second-Generation Robot for Operating Room

Based on the results from the prototype robot, a more advanced robot was designed (Fig. 11). This second-generation robot was designed for use in the operating room. Considering the limited space over patient's head during operations, we chose a small and compact parallel robot design. The parallel robot we designed has 6 actuators that manipulate its moving platform through 6 independently controlled linear actuators (cylinders). The base of this robot is held stationary during surgery through mechanical lock. The steerable electrode is held on the moving platform.

The overall dimensions of the robot are shown in Figure 12. The diameters of the moving platform and the base platform are ∅75 and ∅95 mm, respectively. The height of the robot (from moving platform to base) is 120 mm at fully retracted status and 180 mm at fully extended position. When holding the electrode, the distance from the tip of the electrode to the moving platform is approximately 90 mm, which allows enough space for safe insertions on adults and children. Upon clinical evaluation in Figure 12, the outer diameter of the electrode holder was

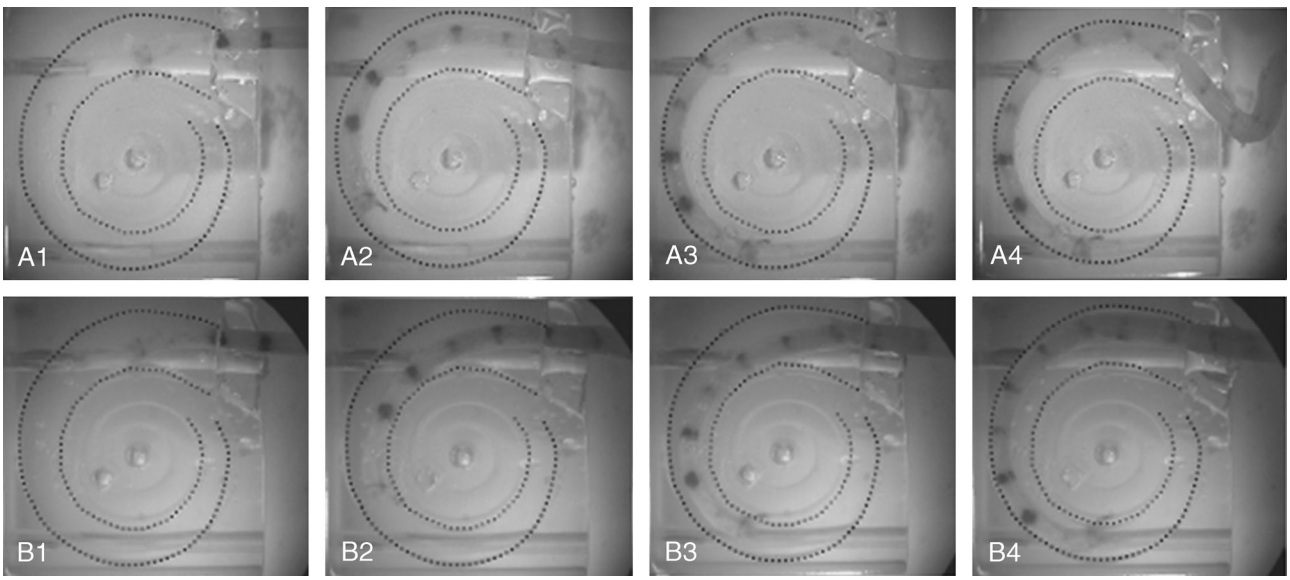

FIG. 10. Robotically inserting straight and steerable electrodes into 3D scala tympani models. *A*, Straight electrode insertion sequential images. *B*, Steerable electrode insertion sequential images.

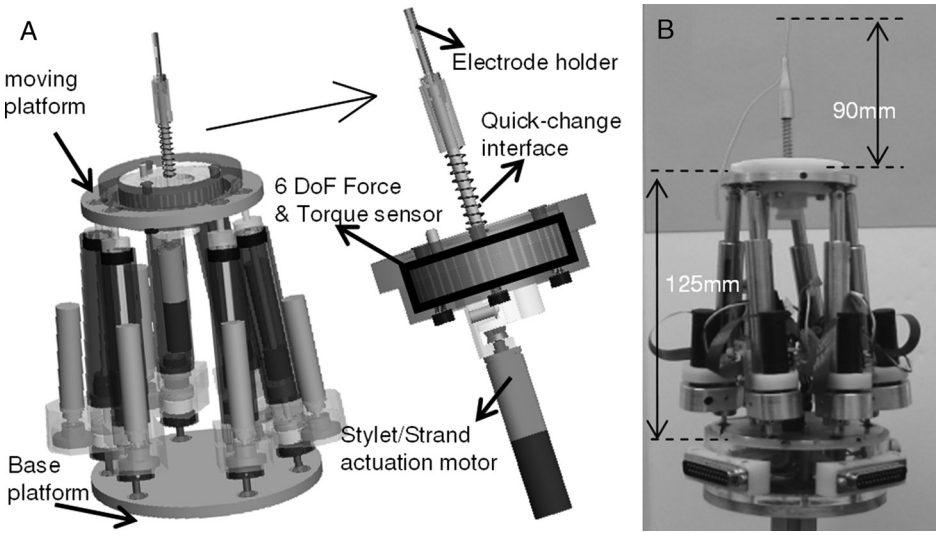

FIG. 11. Second-generation robot design.

changed from ∅5.0 to ∅2.0 mm, and it was redesigned to hold various types of electrode arrays.

One additional motor is used to control the pull on the strand/stylet when using steerable electrode or perimodiolar electrode. A Nano43 force sensor (ATI Industrial Automation, Apex, NC, USA), capable of detecting spatial forces (±0.1 g) and moments (±0.01 Nmm) in any directions, is mounted on the moving platform connected to the electrode holder through a quick-change interface. The plastic quick-change interface holds the force sensor in position. The strand/stylet will be passed through the electrode holder and connected to the actuation motor under the quick-change interface. The electrode holder and the interface are designed to be disposable while the robot with the force sensor will be covered by a sterile draping during surgery.

A desktop prototype of the complete robot-assisted cochlear implant surgery system is demonstrated in Figure 13. The robot is able to move at a maximal speed of 5.7 mm/s in space, which is enough for typical electrode insertions. A Phantom Omni haptic device (SensAble Technologies, Inc., Woburn, MA, USA) is used to control the robot. This joystick allows surgeons to move the robot, following the hand motions of surgeons. The computer shows and records the surgery information, such as insertion depth, insertion speed, and sensed force.

Three levels of safety features have been implemented on this robot. The first level lies on the software. The robot can be disabled by software when an unexpected situation occurs. One additional safety feature is added to the control mechatronics. Each actuator of this robot can be disabled separately if it is not functioning correctly. The highest level of safety is achieved by the external emergency stop. It is available for surgeons to manually stop the whole system in case the insertion needs to be interrupted.

DISCUSSIONS

Robotic insertion simulations and experiments showed that steerable electrode array insertions using a more advanced robot lead to smaller electrode insertion forces. Although the robotic insertion strategy is effective, our

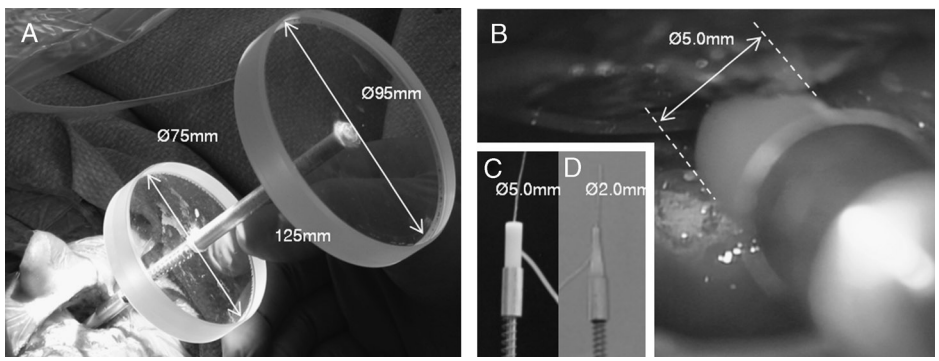

FIG. 12. Second-generation robot dimensions. *A*, Real-size robot mockup demonstration tested in real surgery. *B*, Original electrode holder dimension (∅5.0 mm) in surgery. *C*, Original electrode holder dimension (∅5.0 mm). *D*, Current electrode holder dimension (∅2.0 mm).

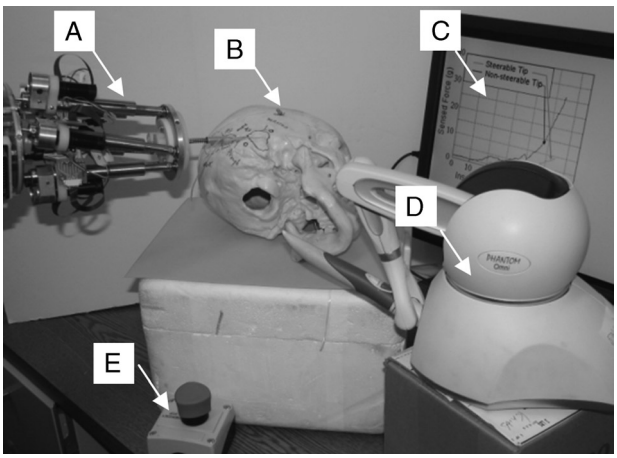

FIG. 13. Robot-assisted cochlear implant operations system setup demonstration. *A*, Insertion robot. *B*, Human skull model. *C*, Force reading/recording PC. *D*, Phantom Omni haptic device. *E*, Emergency stop.

fabrication techniques and laboratory equipments limited our ability to manufacture better electrodes and demonstrate better results in simulation and experiments. For example, in Figure 7, the bent electrode shapes using 4 DoF insertion (Fig. 7B, C, and H) still does not match the scala tympani curve as perfectly as the others. This is due to the fact that the bending characteristics of that particular electrode cannot change any more once it is fabricated. If we were able to fabricate an electrode such that its bent shapes match the scala tympani curve perfectly at different insertion depths, it would result in even better insertions.

Less trauma to the cochlea and electrode precise placement is the goal for every cochlear implant surgery. Our parallel robot aims to help surgeons improve surgical outcomes and reduce overall surgical operation time. By improving surgical outcomes and reducing cochlear trauma ultimately, the systems described in this work may provide us with the necessary tools to reliably preserve residual hearing during cochlear implantation. The robot with the force sensor and the controller will be stored in the operating room. The electrodes together with the quick-change interface will be prepackaged with other surgical tools. Before surgeries, surgeons only need to snap on the interface to the robot moving platform and connect the strand/stylet to the actuation motor. Then, the robotic system is ready for insertions. After insertions, surgeons need to remove the electrode holder from the electrode and fix the actuation strand or remove the stylet.

Our future work will focus on temporal bone studies using this second-generation robot to validate clinical viability before in vivo trials.

CONCLUSION

This article presents preliminary results on robot-assisted cochlear implant surgery. A prototype robot was used together with a steerable electrode prototype to experimentally validate the assumption that robotic assistance can help reduce insertion forces. Based on the data collected from the experiments, a second-generation medical robot is designed specifically for cochlear implant surgery. This robot combines with a high-precision force sensor and a user interface with force feedback. Surgeons can use the user interface to control the insertion process, and sensed insertion force can be automatically recorded through the force sensor and reflected to the user via force feedback. A disposable quick-change interface is designed to hold different types of electrode. These features of the robot prepare it for tests on temporal bones. Further work on sterilization through the use of draping and additional software and hardware safeguards will allow the use of this robot in a clinical setting (26,27).

Acknowledgment: The authors gratefully acknowledge National Science Foundation for their research funding.

REFERENCES

1. Gantz B, Turner C, Gfeller K, et al. Preservation of hearing in cochlear implant surgery: advantages of combined electrical and acoustical speech processing. *Laryngoscope* 2005;115:796–802.
2. Aschendorff A, Kromeier J, Klenzner T, et al. Quality control after insertion of the nucleus contour and contour advance electrode in adults. *Ear Hear* 2007;28:75S–9S.
3. Gantz BJ, Hansen MR, Turner CW, et al. Hybrid 10 clinical trial: preliminary results. *Audiol Neurootol* 2009;14:32–8.
4. Todd CA, Naghdy F, Svehla MJ. Force application during cochlear implant insertion: an analysis for improvement of surgeon technique. *IEEE Trans Biomed Eng* 2007;54:1247–55.
5. Zhang J, Bhattacharyya S, Simaan N. Model and parameter identification of friction during robotic insertion of cochlear-implant electrode arrays. *IEEE Trans Rob Autom* 2009;3859–64.
6. Juvinall R, Marshek K. *Fundamentals of Machine Component Design*. New York, NY: John Wiley & Sons, Inc, 2005;735–7.
7. Eshraghi AA, Yang NW, Balkany TJ. Comparative study of cochlear damage with three perimodiolar electrode designs. *Laryngoscope* 2003;113:415–9.
8. Adunka O, Gstoettner W, Hambek M, et al. Preservation of basal inner ear structures in cochlear implantation. *J Otorhinolaryngol Head Neck Surg* 2004;66:306–12.
9. Adunka O, Kiefer J, Unkelbach MH, et al. Development and evaluation of an improved cochlear implant electrode design for electric acoustic stimulation. *Laryngoscope* 2004;114:1237–41.
10. Wardrop P, Whinney D, Rebscher SJ, et al. A temporal bone study of insertion trauma and intracochlear position of cochlear implant electrodes. I: Comparison of Nucleus banded and Nucleus Contour(TM) electrodes. *Hear Res* 2005;203:54–67.
11. Roland JT. A model for cochlear implant electrode insertion and force evaluation: results with a new electrode design and insertion technique. *Laryngoscope* 2005;15:1325–39.
12. Cohen NL, Roland JT, Fishman A, et al. Surgical technique for the Nucleus Contour cochlear implant. *Ear Hear* 2002;23:59S–66S.
13. AOS Insertion Tool for the Nucleus 24 Contour Advance cochlear implant. Available at: http://www.designawards.com.au/application_detail.jsp?applicationID=1746. Accessed October 1, 2009.
14. Howe RD, Matsuoka Y. Robotics for surgery. *Ann Rev Biomed Eng* 1999;1:211–40.
15. Taylor RH, Stoianovici D. Medical robotics in computer-integrated surgery. *IEEE Trans Rob Autom* 2003;19:765–81.
16. Majdani O, Rau T, Baron S, et al. A robot-guided minimally invasive approach for cochlear implant surgery: preliminary results of a temporal bone study. *Int J Comp Assist Radiol Surg* 2009;4:475–86.

17. Coulson CJ, Reid AP, Proops DW, et al. ENT challenges at the small scale. *Int J Med Rob Comp Assist Surg* 2007;3:91–6.
18. Frederick RL, Jack HN, Benoit MD, et al. Clinical validation of percutaneous cochlear implant surgery: initial report. *Laryngoscope* 2008;118:1031–9.
19. Matsumoto N, Hong J, Hashizume M, et al. A minimally invasive registration method using surface template-assisted marker positioning (STAMP) for image-guided otologic surgery. *Otolaryngol Head Neck Surg* 2009;140:7.
20. Zhang J, Xu K, Simaan N, et al. A pilot study of robot-assisted cochlear implant surgery using steerable electrode arrays. *Med Image Comp Comput Assist Interv* 2006;9:33–40.
21. Zhang J, Roland JT, Manolidis S, et al. Optimal path planning for robotic insertion of steerable electrode arrays in cochlear implant surgery. *ASME J Med Device* 2009;3:011001–10.
22. Chen B, Kha H, Clark G. Development of a steerable cochlear implant electrode array. *3rd Kuala Lumpur International Conference on Biomedical Engineering* 2007;607–10.
23. Hussong A, Rau T, Ortmaier T, et al. An automated insertion tool for cochlear implants: another step towards atraumatic cochlear implant surgery. *Int J Comput Assist Radiol Surg* 2010;5:163–71.
24. Cohen L, Xu J, Xu SA, et al. Improved and simplified methods for specifying positions of the electrode bands of a cochlear implant array. *Am J Otol* 1996;17:859–65.
25. Ketten DR, Skinner MW, Wang G, et al. In vivo measures of cochlear length and insertion depth of nucleus cochlear implant electrode arrays. *Ann Otol Rhinol Laryngol* 1998;175:1–16.
26. Yoo SK, Wang G, Rubinstein JT, et al. Three-dimensional modeling and visualization of the cochlea on the internet. *IEEE Trans Inf Technol Biomed* 2000;4:144.
27. Wysocki J. Dimensions of the human vestibular and tympanic scalae. *Hear Res* 1999;135:39–46.